

Physics from Photons at the LHC

Lucian Harland-Lang¹

¹ University of Oxford, Rudolf Peierls Centre, Beecroft Building, Parks Road, Oxford, OX1 3PU lucian.harland-lang@physics.ox.ac.uk

July 20, 2021



*Proceedings for the XXVIII International Workshop
on Deep-Inelastic Scattering and Related Subjects,
Stony Brook University, New York, USA, 12-16 April 2021*
doi:[10.21468/SciPostPhysProc.7](https://doi.org/10.21468/SciPostPhysProc.7)

Abstract

LHC collisions can act as a source of photons in the initial state. This mechanism plays an important role in the production of particles with electroweak couplings, and a precise account of photon-initiated (PI) production at the LHC is a key ingredient in the LHC precision physics programme. I will discuss the possibility of modelling PI processes directly via the structure function approach. This can provide percent level precision in the production cross sections, and is therefore well positioned to account for LHC precision requirements. This formalism in addition allows one to make use of another useful feature of photons, namely that they are colour-singlet and can often be emitted elastically (or quasi-elastically) from the proton. I will discuss recent work on applications of the structure function approach to precision calculations of PI production in the inclusive mode, and to ‘exclusive’ processes with rapidity gaps, which can provide a unique probe of the Standard Model and physics beyond it.

Contents

1	Introduction	1
2	The Structure Function Approach and inclusive photon-initiated production	2
3	Modelling (semi)-exclusive photon-initiated production	4
4	Conclusion	4
References		5

1 Introduction

A major aim of the LHC, and the HL-LHC upgrade that will follow, is to precisely test the Standard Model (SM) predictions for as wide a range of collider processes as possible. A

27 particularly important element of this involves events with leptons in the final state, which
 28 play a key role in determinations of the weak mixing angle, $\sin^2 \theta_W$, the W boson mass, M_W ,
 29 and constraints on the proton PDFs. A key ingredient in this is the availability of high precision
 30 theoretical predictions for the SM processes, an important element of which is the contribution
 31 from the photon-initiated (PI) channel.

32 A further feature of this channel in proton-proton collisions is that the colour singlet pho-
 33 ton exchange naturally leads to exclusive events, where the photons are emitted elastically
 34 from the protons. This is particularly relevant in the context of the dedicated forward pro-
 35 ton detectors at the LHC, namely AFP and CT-PPS, which have been installed in association
 36 with both ATLAS and CMS, respectively [5]. More generally, even if the initial-state photon
 37 is emitted inelastically, there is no colour flow as a result, and there is still a possibility for
 38 semi-exclusive events with rapidity gaps in the final-state between the proton dissociation
 39 system(s) and the centrally produced object. Indeed, a range of data have been collected
 40 using this technique at the LHC [6].

41 Here, we present the application of the so-called structure function (SF) method to the
 42 calculation of both the PI component of inclusive lepton production, at high precision, and PI
 43 production in the exclusive mode.

44 2 The Structure Function Approach and inclusive photon-initiated 45 production

46 The SF framework is a rather useful method [1,2] for calculating the PI lepton pair production
 47 cross section directly in terms of the proton structure functions. For processes such as (off Z -
 48 peak) lepton pair production this provides percent precision in the predicted cross sections,
 49 with no accompanying factorization scale variation uncertainty, as is present in the calculation
 50 within collinear factorization.

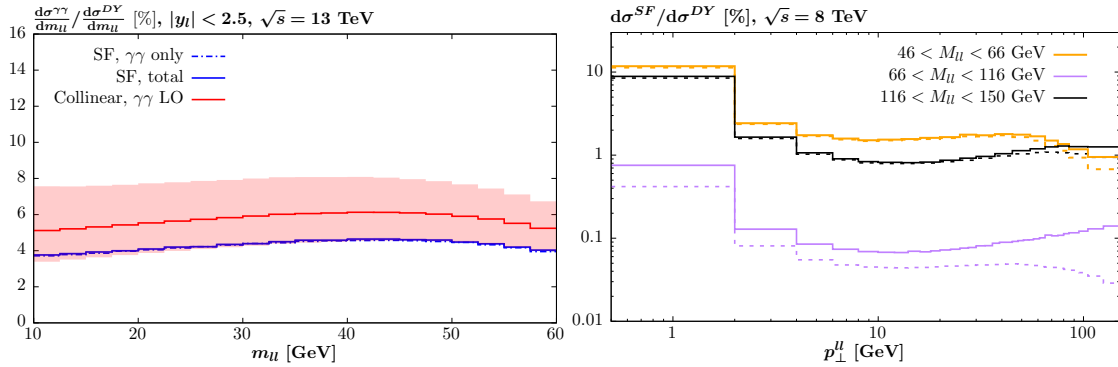


Figure 1: (Left) Ratio of the PI cross sections for lepton pair production to the NLO QCD Drell-Yan cross section at the 13 TeV LHC. The LO collinear predictions (including scale variation uncertainties) and the structure function result are shown, in the latter case for both the pure $\gamma\gamma$ initiated and the total. (Right) Percentage contribution from PI production to the lepton pair p_\perp distribution, within the ATLAS [3] off-peak event selection, at 8 TeV. The QCD predictions correspond to NNLO + NNLL QCD theory [4]. The total (pure $\gamma\gamma$) contributions are shown by the solid (dashed) lines.

51 In the SF approach, the PI cross section is given by

$$\sigma_{pp} = \frac{1}{2s} \int \frac{d^3p_1 d^3p_2 d\Gamma}{E_1 E_2} \alpha(Q_1^2) \alpha(Q_2^2) \frac{\rho_1^{\mu\mu'} \rho_2^{\nu\nu'} M_{\mu'\nu'}^* M_{\mu\nu}}{q_1^2 q_2^2} \delta^{(4)}(q_1 + q_2 - k). \quad (1)$$

52 Here the outgoing hadronic systems have momenta $p_{1,2}$ and the photons have momenta $q_{1,2}$,
 53 with $q_{1,2}^2 = -Q_{1,2}^2$. We consider the production of a system of 4-momentum $k = q_1 + q_2 = \sum_{j=1}^N k_j$
 54 of N particles, where $d\Gamma = \prod_{j=1}^N d^3k_j / 2E_j (2\pi)^3$ is the phase space volume. $M^{\mu\nu}$ corresponds
 55 to the $\gamma\gamma \rightarrow X(k)$ production amplitude, with arbitrary photon virtualities. ρ is the density
 56 matrix of the virtual photon, which is given in terms of the well known proton structure func-
 57 tions, see [1, 2] for an explicit expression and [2] for the extension to include initial-state Z
 58 bosons.

59 A representative selection of results are shown in Fig. 1. In the left plot we show the lepton
 60 pair invariant mass distribution, plotting the ratio of the PI contribution to the NLO QCD Drell-
 61 Yan cross section at the 13 TeV LHC. For this choice of cuts, the PI component is at the $\sim 4\%$
 62 level, and hence is small but certainly not negligible. We note that the solid curve includes
 63 the uncertainty due to the experimental determination of the structure functions, but this is
 64 so small as to not be visible on the plot. The ‘total’ contribution includes initial-state Z boson,
 65 and mixed $\gamma/Z + q$ contributions, but these are found to give a negligible contribution. The LO
 66 collinear result is also shown for comparison. This is seen to lie above the SF results, though
 67 consistent within the large scale variation uncertainties; clearly, one should work at least at
 68 NLO when applying the collinear approach. However, for the present observable we can see
 69 that the SF approach provides percent level precision already.

70 Above the Z peak (not shown here), the PI contribution is as large as $\sim 10\%$, and can
 71 again be predicted with high precision by the SF approach. As discussed in further detail
 72 in [2], these results imply that the PI contribution to the dilepton $\cos\theta^*$ distribution, which
 73 is used for determinations of $\sin^2\theta_W$ as well as PDF constraints, can also be highly relevant.
 74 Detailed comparisons are presented in [2] and this is indeed found to be the case, with the SF
 75 approach providing high precision predictions for the PI contribution.

76 As the SF formulation of Eq. 1 is provided differentially with respect to the photon vir-
 77 tualities, Q^2 , we can also readily provide predictions with respect to the dilepton transverse
 78 momentum, p_{\perp}^{ll} . In Fig. 1 (right) we show the ratio of the PI contribution to NNLO+N³LL
 79 resummed QCD predictions produced with NNLOjet+RadISH [4]. The total (solid) curve in-
 80 cludes mixed $\gamma + q$ diagrams, which will be sensitive to resummation effects in the low p_{\perp}^{ll}
 81 region, not included here, is only shown for rough guidance in this region. Focussing on the
 82 pure $\gamma\gamma$ component, i.e. the dashed lines, one can see a significant enhancement observed
 83 in the pure $\gamma\gamma$ contribution in the lower $0 < p_{\perp}^{ll} < 2$ GeV region. This is explained in part
 84 by the Sudakov suppression in the QCD contribution in this region, which is absent in the $\gamma\gamma$
 85 channel. However, another key factor in this is that the $\gamma\gamma$ cross section is particularly peaked
 86 in this region, due to the significant contribution from elastic photon emission. This elastic
 87 component, or indeed the low Q^2 resonant and non-resonant components, are not modelled
 88 differentially in a pure collinear calculation, and hence the SF calculation is particularly well
 89 suited to deal with this very low p_{\perp}^{ll} region. As explored in [2], this could have implications
 90 for experimental determinations of M_W , through the tuning that is done to the low p_{\perp}^{ll} region
 91 of dilepton production.

92 Finally, we note that the benefit of applying the SF approach directly, while transparent
 93 for process where the final state of interest (l^+l^- , W^+W^- ...) is directly produced by the $\gamma\gamma$
 94 initial state, is less clear in the mixed $\gamma + q$ case. Here, one must deal with the collinear en-
 95 hancement of the $\gamma \rightarrow q\bar{q}$ splitting, and at this level of precision include QED DGLAP evolution
 96 of the quark/antiquark PDFs, which certainly requires one introduce a photon PDF within the
 97 LUXqed approach. Further discussion can be found in [2].

3 Modelling (semi)–exclusive photon–initiated production

This theoretical treatment of exclusive and semi–exclusive events is rather distinct from the standard inclusive case. The reasons for this are twofold: first, if events are selected with a rapidity veto than the case where decay products from the proton dissociation system enter the veto region must be excluded, and second, there may be additional inelastic proton–proton QCD interactions (in other words, underlying event activity) that fill the gap region. The latter effect must be accounted for via the so–called ‘survival factor’ probability of no additional proton–proton interactions [7], while the former requires a fully differential treatment of the PI process, including a MC implementation such that the showering and hadronisation of the dissociation system may be accounted for.

In [6], we presented such a MC implementation, SuperChic 4, for the case of lepton pair production. This makes use of the SF approach, to provide a high precision prediction for the underlying PI process that is fully differential in the kinematics of the final–state protons and/or dissociation systems. This can then be interfaced to a general purpose MC for further showering/hadronization; we make use of Pythia 8.2 [8]. We in addition account for the survival factor, in a manner that take full account of the dependence of this quantity on the event kinematics and the specific channel (elastic or inelastic). SuperChic 4 is the first generator of its kind to take account of all of these features, which are essential when providing results for semi–exclusive PI production.

In Fig. 2 (left) we show the predicted survival factor as a function of the dimuon invariant mass, at $\sqrt{s} = 13$ TeV. We can see that broadly there is a large difference in the magnitude of the survival factor between the DD and elastic/SD cases, with the former being significantly smaller. This is driven by the fact that in the DD case the photon Q^2 is generally much higher, and so the collision is less peripheral in terms of the impact parameter of the colliding protons; the most peripheral elastic interaction has the highest survival factor. We can also see that as the invariant mass increases, the survival factor decreases, due to effect of the kinematic requirement for producing an on-shell proton at the elastic vertex for larger photon momentum fractions, which implies a larger photon Q^2 . For the DD case the survival instead increases somewhat, due to the smaller phase space in photon Q^2 at the highest M_{ll} values. These are examples of a broader result, namely that the survival factor is not a single constant value, but rather depends sensitively on the process and kinematics.

In Fig. 2 (right) we show a comparison of the predicted acoplanarity distribution for muon pairs to the ATLAS data on semi–exclusive dilepton production at $\sqrt{s} = 7$ TeV [9]. The theory result includes the impact of the rapidity veto that is applied in order to selected these events, as well as the survival factor (we show results without this included for comparison). We can see that the distribution is described rather well once the survival factor is included.

4 Conclusion

In summary, PI production is a rather unique channel at the LHC that plays a key role in both inclusive and exclusive particle production. We have presented state–of–the–art results for dilepton production in both of these channels, including MC implementations; SFGen [2] and SuperChic 4 [6] for inclusive and exclusive production, respectively.

Funding information I thank the Science and Technology Facilities Council (STFC) for support via ST/L000377/1.

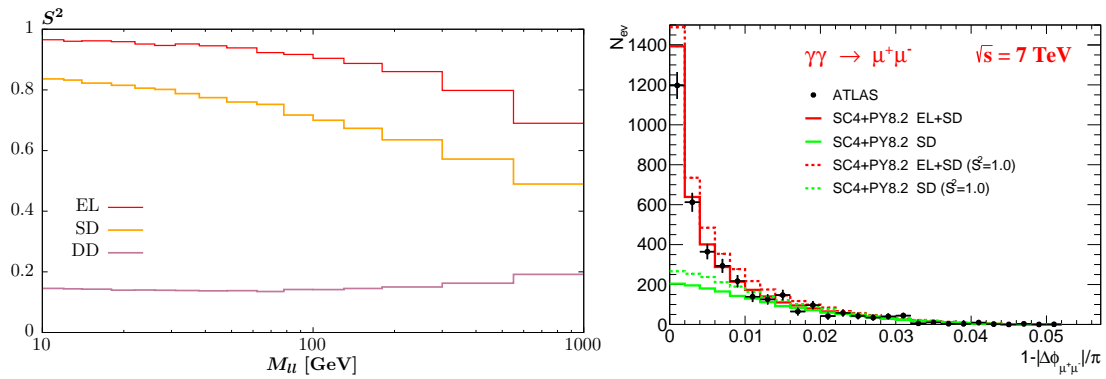


Figure 2: (Left) Soft survival factor for lepton pair production as a function of the invariant mass, M_{ll} , of the dilepton system. (Right) Comparison of SuperChic 4 + Pythia 8.2 predictions for the dilepton acoplanarity distribution compared to the ATLAS data [9] at $\sqrt{s} = 7$ TeV, within the corresponding experimental fiducial region, and with a rapidity veto applied on tracks in the central region. Results without the soft survival factor included are shown in addition.

141 References

- 142 [1] L. Harland-Lang, *The Proton in High Definition: Revisiting Photon-Initiated Production in*
 143 *High Energy Collisions*, JHEP **03**, 128 (2020), doi:[10.1007/JHEP03\(2020\)128](https://doi.org/10.1007/JHEP03(2020)128), [1910.10178](https://arxiv.org/abs/1910.10178).
 144
- 145 [2] L. A. Harland-Lang, *Physics with Leptons and Photons at the LHC* (2021), [2101.04127](https://arxiv.org/abs/2101.04127).
- 146 [3] G. Aad *et al.*, *Measurement of the transverse momentum and ϕ_η^* distributions of Drell–Yan*
 147 *lepton pairs in proton–proton collisions at $\sqrt{s} = 8$ TeV with the ATLAS detector*, Eur. Phys. J. C **76**(5), 291 (2016), doi:[10.1140/epjc/s10052-016-4070-4](https://doi.org/10.1140/epjc/s10052-016-4070-4), [1512.02192](https://arxiv.org/abs/1512.02192).
 148
- 149 [4] W. Bizoń, X. Chen, A. Gehrmann-De Ridder, T. Gehrmann, N. Glover, A. Huss, P. F. Monni,
 150 E. Re, L. Rottoli and P. Torrielli, *Fiducial distributions in Higgs and Drell-Yan production at*
 151 *$N^3LL+NNLO$* , JHEP **12**, 132 (2018), doi:[10.1007/JHEP12\(2018\)132](https://doi.org/10.1007/JHEP12(2018)132), [1805.05916](https://arxiv.org/abs/1805.05916).
- 152 [5] C. Royon and N. Cartiglia, *The AFP and CT-PPS projects*, Int.J.Mod.Phys. A **29** (2014) 28,
 153 1446017 (2015), [1503.04632](https://arxiv.org/abs/1503.04632).
- 154 [6] L. Harland-Lang, M. Tasevsky, V. Khoze and M. Ryskin, *A new approach to modelling elastic*
 155 *and inelastic photon-initiated production at the LHC: SuperChic 4*, Eur. Phys. J. C **80**(10),
 156 925 (2020), doi:[10.1140/epjc/s10052-020-08455-0](https://doi.org/10.1140/epjc/s10052-020-08455-0), [2007.12704](https://arxiv.org/abs/2007.12704).
- 157 [7] L. A. Harland-Lang, V. A. Khoze, M. G. Ryskin and W. Stirling, *Central exclusive pro-*
 158 *duction within the Durham model: a review*, Int.J.Mod.Phys. A **29**, 1430031 (2014),
 159 doi:[10.1142/S0217751X14300312](https://doi.org/10.1142/S0217751X14300312), [1405.0018](https://arxiv.org/abs/1405.0018).
- 160 [8] T. Sjöstrand, S. Ask, J. R. Christiansen, R. Corke, N. Desai, P. Ilten, S. Mrenna, S. Prestel,
 161 C. O. Rasmussen and P. Z. Skands, *An introduction to PYTHIA 8.2*, Comput. Phys. Commun.
 162 **191**, 159 (2015), doi:[10.1016/j.cpc.2015.01.024](https://doi.org/10.1016/j.cpc.2015.01.024), [1410.3012](https://arxiv.org/abs/1410.3012).
- 163 [9] G. Aad *et al.*, *Measurement of exclusive $\gamma\gamma \rightarrow \ell^+\ell^-$ production in proton-proton collisions*
 164 *at $\sqrt{s} = 7$ TeV with the ATLAS detector* (2015), [1506.07098](https://arxiv.org/abs/1506.07098).